

Geochemical Activity of Faults in the Baikal Rift Zone (Mercury, Radon, and Thoron)

P. V. Koval^a, Yu. N. Udodov^a, V. A. San'kov^b, A. A. Yassenovskii^a, and L. D. Andrulaitis^a

Presented by Academician F.A. Letnikov July 11, 2005

Received August 25, 2005

DOI: 10.1134/S1028334X06060171

Geochemically active faults are accompanied by emission of matter into the host rocks and atmosphere [1]. In particular, they include active faults of volcanic and rift zones accompanied by elevated heat flow, volcanism, thermal springs, and gas emission. A part of the emitted components (in particular, Hg, S, trace elements, and others) is a priori considered juvenile products [2–4].

The high seismicity and thermal and hydrothermal activity make the Baikal Rift Zone (BRZ) an ideal object for study of geochemical activity and, in particular, the “mercury breath” of faults. We carried out a long-term decadal monitoring of Hg concentration at the mouth of the Angara River (intersection of the active Obruchev and Angara faults [5]). The results obtained confirmed the inferred correlation [6] of Hg contents in water at the junction of two deep faults (Fig. 1) with seismic activity. Owing to technical and analytical difficulties in organizing continuous monitoring of gas emission in the fault zones, we investigated the Hg content in soil profiles across the fault zones (Fig. 1). It was assumed that the humus material can be used as a natural sorbent—the indicator of Hg partial pressure in an emission flux—because of its high sorption potential (including chemisorption [8]). This is confirmed by the positive correlation between contents of Hg and organic matter (C_{org}) in humus horizon (A) in the background areas ($K = 0.57–0.97$). Therefore, most samples were taken from the humus horizon. Taking into consideration fairly wide variations of C_{org} in horizon A (0.32–34.4%), the measured Hg contents were normalized to C_{org} to decrease the effect of variations of humus

contents in various soil samples. The measurement sites were usually established on both sides of the fault plane beginning from the seismic dislocation point with a spacing of ~50 m gradually increasing to 1–2 km in the inferred background area. The Hg content was determined on ARF-1M and AFS PSSA 10.023 Merlin mercury analyzers with a detection limit of 0.002 mg/kg. In some profiles, we determined the Hg content in soil air with an AGP-01 portable gas–mercury analyzer. Soil sampling was accompanied by measurements of radon and thoron activity in soil air by a RGA-01 radiometer using standard technique.

Judging from [9], the modal value of total sampling of mercury measurements (0.016 mg/kg, $n = 220$), and the results obtained on the most complete profiles (Arshan and Sakhuli), the background Hg content in the humus soil horizon of the Baikal area varies from <0.016 to 0.029 mg/kg. The background Hg content normalized to organic carbon is $\sim 0.01 \cdot 10^{-3}$. The modal values obtained in our measurements (3200 and 15 900 Bq/m³) were accepted as background Rn and Tn contents, respectively. The background Rn/Tn ratio is ~ 0.2 .

The anomalies of Hg and radioactive gases of different intensities were found in soils above all studied faults regardless of their morphology and genesis (table). They typically have a complex shape with several maximums, presumably reflecting uneven activation of local fault planes (Fig. 2). Simple anomalies with peaks located above the major seismic dislocation are less common. The intensity of anomalies varies along the fault strike. The position of anomalous peaks does not universally coincide with the major fault plane shown on geological maps. In some cases, they correspond to faults overlain by loose sediments. The maximums of various anomalies (Hg in soil, Hg in soil air, and Rn and Tn in soil) in the fault zones are typically slightly displaced with respect to each other.

Data presented in the table indicate that the intensities of anomalies related to deep faults of various types show no significant differences, with the exception of

^a Vinogradov Institute of Geochemistry and Analytical Chemistry, Siberian Division, Russian Academy of Sciences, ul. Favorskogo 1a, Irkutsk, 664033 Russia; e-mail: koval@igc.irk.ru

^b Institute of the Earth's Crust, Siberian Division, Russian Academy of Sciences, ul. Lermontova 128, Irkutsk, 664033 Russia; e-mail: sankov@crust.irk.ru

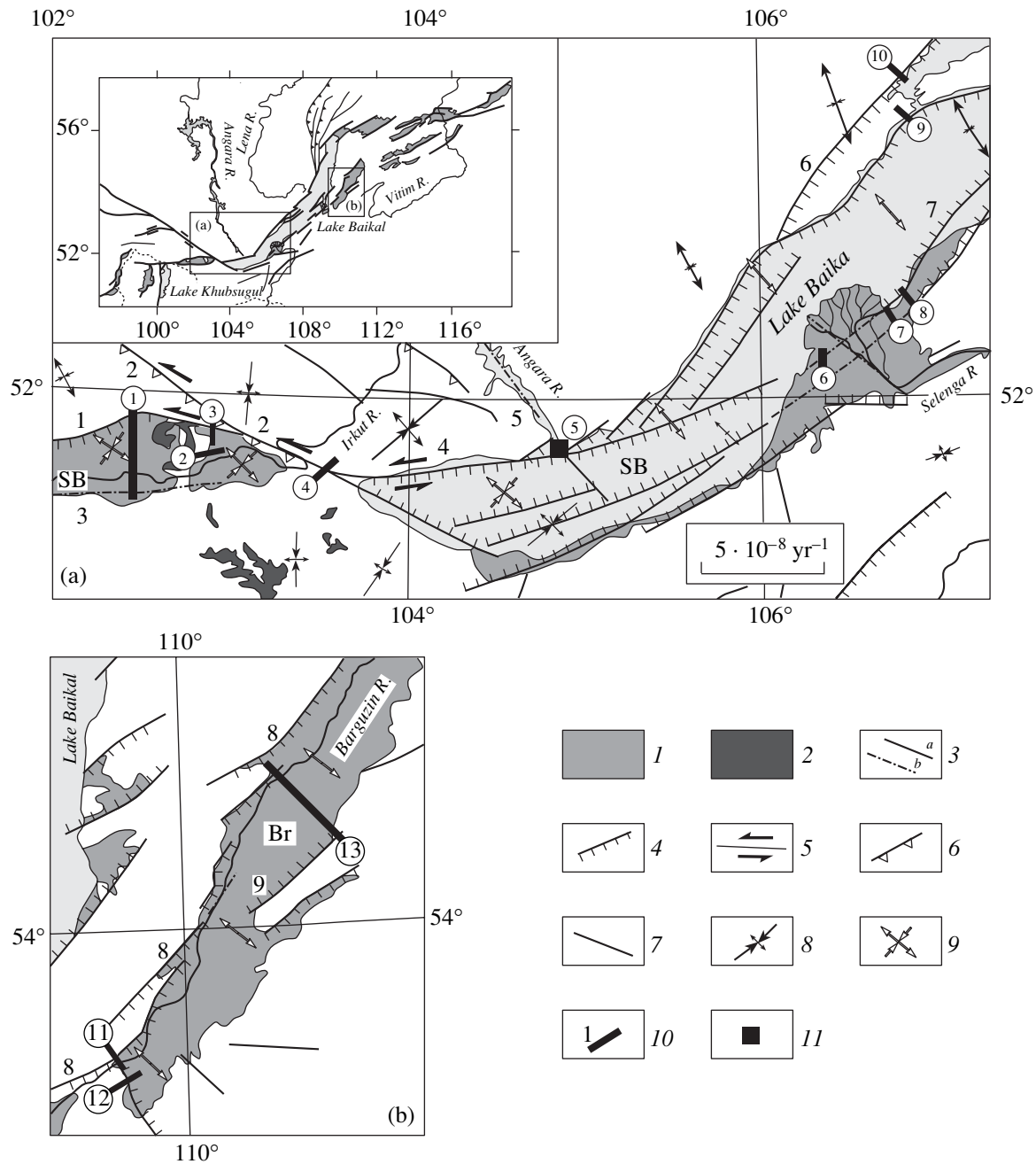


Fig. 1. Sketch map of faults and profiles. Inset shows the positions of study areas in the Baikal rift system. (1) Cenozoic sediments of rift depressions: (Tn) Tunka, (SB) South Baikal, (Br) Barguzin; (2) Cenozoic basalts; (3) neotectonic faults: (a) proved, (b) inferred; (4–7) kinematic types of faults: (4) normal; (5) strike-slip; (6) reverse; (7) unspecified type; (8, 9) modern tectonic deformations: (8) based on GPS geodesy (scale is shown in the figure) [7], (9) based on calculations of seismotectonic deformations [7]; (10) reference profiles (encircled numbers): (1) Arshan, (2) Guzhiry, (3) Samsaltyi, (4) Anchuk, (5) Angara River head (monitoring site), (6) Selenga, (7) Sharashevo, (8) Oimur, (9) Orso, (10) Sarma, (11) Gremyachaya, (12) Shapen'kovo, (13) Sakhuli Argada; (11) site of all-the-year-round hydrochemical monitoring of water (Angara River head). Faults: (1) Tunka, (2) Main Sayan, (3) North Khamar Daban, (4) Obruchev, (5) Angara, (6) Primorskii, (7) Del'tovyi, (8) Barguzin, (9) Argada.

certain anomalies in the Barguzin fault zone. This fact presumably testifies to a complex change in geochemical activity of the faults with time.

The results make it possible to outline a set of characteristics (boundary conditions) of the preliminary

conceptual model of the “mercury breath” of the BRZ. Active faults of the BRZ are accompanied by Hg anomalies in water, soil, and soil and near-surface air. The anomalies are associated with active faults (including low-active transverse structures) that differ in morphology, genesis, and thermal activity. The intensity and

Characteristics of major faults of the BRZ and related anomalies of mercury, radon, and thoron

Fault, profile (Fig. 1)	Type of strained state (kinematics)	Heat flow, mW/m ² [10]	\dot{e}_{\max} Hg, mg/kg	K_k Hg	Rn, activity, Bq/m ³	Tn, \ddagger activity, Bq/m ³
Main active structures: Angara (5) + Obruchev (4), Angara River head monitoring site	Extension (normal fault)	$\frac{40}{53}$	0.000027 (0.000167)	–	–	–
Main Sayan general fault (2), Anchuk profile	Transpression (reverse strike-slip fault)	$\frac{40}{50}$	0.235	4.1	$\frac{3500}{11600}$	$\frac{12000}{46450}$
Primorskii general fault (1), Sarma profile, Orso profile	Extension (normal fault)	$\frac{50}{59}$	0.050 0.140	3.0 2.7	$\frac{5850}{96200}$	$\frac{25100}{5136601}$
Tunka general fault (1), Arshan profile, Samsaltyi profile	Shear (strike-slip)	$\frac{50}{146}$	0.125	2.0	$\frac{5700}{13600}$	$\frac{15900}{72700}$
			0.175	4.7	$\frac{1650}{4400}$	$\frac{11000}{23200}$
Barguzin general fault (8), Sakhuli profile, Gremyachaya profile	Extension (normal fault)	$\frac{50}{119}$	0.048	8.0	$\frac{3700}{3750}$	$\frac{17100}{26100}$
			0.141	4.6	$\frac{3300}{8900}$	$\frac{17350}{51300}$
Argada (Bayangol) regional fault (9), Sakhuli profile	Extension (normal fault)	–	0.029	3.8	$\frac{3700}{24000}$	$\frac{17100}{41700}$
North Khamar Daban fault (3), Arshan profile	Shear (strike-slip)	–	0.044	2.4	$\frac{5700}{10600}$	$\frac{15900}{26600}$
Del'tovyi (6), Selenga profile, Oimur profile (Proval-2), Sherashevo profile (Proval)	Extension (normal fault)	–	–	–	$\frac{6450}{31850}$	$\frac{25050}{55200}$
			0.047	3.8	$\frac{900}{7000}$	$\frac{1300}{12200}$
			0.036	4.1	$\frac{6250}{2400}$	$\frac{30380}{38500}$
Sherashevo profile (Proval), Transverse low-active structures: Elovsk intradepressional bridge (Tunka depression), Guzhiry profile, Barguzin intradepressional bridge, (Barguzin depression), Shapen'kovo profile	Shear, Extension	–	0.040	4.7	$\frac{1500}{8350}$	$\frac{10750}{14100}$
			0.110	4.5	$\frac{5200}{8250}$	$\frac{35900}{79300}$

Note: Background and maximum anomalous values are given in numerator and denominator, respectively. (C_{\max}) the maximum Hg concentration in the humus soil horizon in the anomaly area of the normalized concentration (mg/kg) and maximum Hg concentration in water of the Angara River head ($\mu\text{g/l}$). The value obtained during a strong cyclone is given in parentheses. (K_k) the maximum concentration coefficient normalized to organic carbon content in the humus horizon relative to local background of the profile.

distribution of emission flows in the fault zones significantly vary in time and space. The Hg flux from faults has a pulsating character due to seismic and, possibly, strong atmospheric perturbations (cyclones). Outbursts related to seismic dislocations can be 20–30 times higher than the background value. The Hg emission from the faults becomes maximal before great seismic events (earthquakes). The background value of fault zone anomalies corresponding to the relative seismic quiescence is 2–10 times higher than that in the adjacent (true background) areas.

Anomalies in the humus horizon presumably correspond to the highest Hg contents in the soil air above faults during their activation. The Hg sorption at the humus barrier is evidently driven by the complexing mechanism [8] with desorption temperatures being enough to retain the absorbed Hg in the temperature field of the earth's surface. The comparison of natural and technogenic anomalies shows that anomalous Hg concentrations are presumably confined to a specific area, which is too far from sorption saturation of the humus barrier [11, 12]. The comparative analysis of

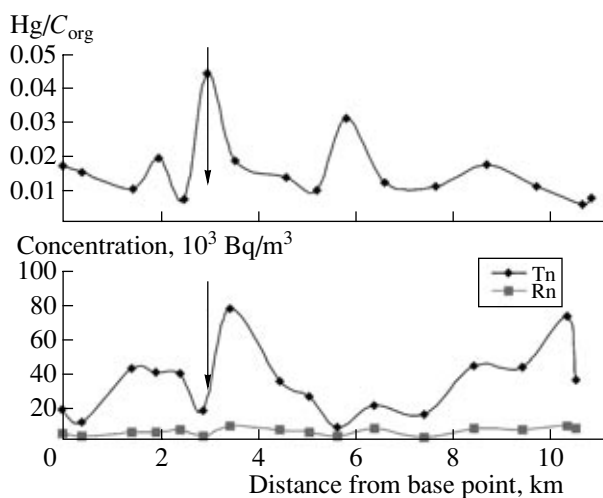


Fig. 2. Distribution patterns of normalized concentrations of Hg in the humus soil horizon, as well as Rn and Tn in soil along the Shapen'kovo profile (Barguzin depression, Fig. 1).

anomalies in soil, water, and air indicates that the absorption isotherm has a comparatively gentle slope under the considered natural conditions.

Hence, based on the comparison of background and anomalous values obtained for various environmental components (soil, soil and near-surface air, and water), the Hg flux from the fault zone can approximately be calculated in the following way:

$F_{\text{Hg}} = K_{\text{fp}}K_{\text{ff}}F_{\text{bz}}$, where F_{Hg} is the Hg emission from a fault zone, F_{bz} is the background flux in the BRZ; K_{ff} is the coefficient accounting for the flux increase in the relatively quiet conditions ("background" flux in the fault); K_{fp} is the coefficient of flux increase during seismic and other perturbations. Based on available data, F_{bz} can be accepted as nearly equal to the regional background ($4\text{g}/\text{km}^2/\text{yr}$ [13]). This is significantly higher than estimates of Baikal evasion ($1.6\text{g}/\text{km}^2/\text{yr}$) [14], which can be considered as the possible lowermost background value. Judging from characteristics of anomalies in soil air, K_{ff} is within 2–10. Based on monitoring data for 1997–2004 [5], the range of K_{fp} of seismic events can be roughly estimated at 1–30.

Thus, emission from fault zones can vary from 3.2–8 to $1200\text{g}/\text{km}^2/\text{yr}$. According to [4, 13, 14], these estimates seem to be plausible. The significant increase (by a few orders of magnitude) of the flux can be anticipated during catastrophic seismic events. This is highly probable, given the fact that Hg fluxes of $\sim 20000\text{g}/\text{km}^2/\text{yr}$ ("Hg-info") were recorded in the Yellowstone Park in 2003 (Abott, 2003).

Knowing the active areas within the rift zone, we can estimate the annual total Hg influx from fault zones. The anomalous intervals account for 15–30% in the profiles intersecting the entire rift depression. Taking the lowest value for calculations, the minimum (quite setting) and maximum values are 170–430 kg

and $\sim 65\text{t}$, respectively. These values are somewhat higher than the natural Hg emission in Siberia [13] and seem to be highly improbable.

ACKNOWLEDGMENTS

This work was supported by the Russian Foundation for Basic Research (project nos. 02-05-65295, 05-05-64626, and 05-05-64702), the Integration Project of the Siberian Division of the Russian Academy of Sciences (project no. 154), and the Russian Academy of Sciences (project no. 13.13).

REFERENCES

1. S. Lombardi, F. Quattrocchi, M. Fytikas, et al., in *Geochemical Seismic Zonation: A Multidisciplinary Approach Using Fluid Geochemistry* (GSZ, 1998), ENV4-T96-0291.
2. N. A. Ozerova, in *Global and Regional Mercury Cycles: Sources, Fluxes and Mass Balances* (Kluwer, Dordrecht, 1996), pp. 463–474 [in Russian].
3. I. I. Stepanov, Extended Abstract of Doctoral Dissertation in Geology and Mineralogy (IMGRE, Moscow, 1996) [in Russian].
4. V. Z. Fursov, *Possibilities of Mercuryometry* (IMGRE, Moscow, 1998) [in Russian].
5. P. V. Koval, Yu. N. Yudodov, L. D. Andrulaitis, et al., *Dokl. Earth Sci.* **389**, 282 (2003) [*Dokl. Akad. Nauk* **389**, 235 (2003)].
6. S. D. Taliev, A. A. Zhdanov, A. A. Fomina, et al., *Volcanol. Seismol.*, No. 6, 133 (1998).
7. V. A. San'kov, A. V. Likhnev, V. I. Melnikova, et al., in *On Use of the Space Techniques for Asia-Pacific Regional Crustal Movements Studies, Int. Seminar APSG, Irkutsk* (GEOS, Moscow, 2002), pp. 118–126 [in Russian].
8. G. M. Varshal, I. Ya. Koshcheeva, S. D. Khushvakhtova, et al., *Geochem. Int.* **37**, 229 (1999) [*Geokhimiya*, No. 3, 269 (1999)].
9. P. V. Koval, G. V. Kalmychkov, V. F. Gelety, et al., *J. Geochem. Explor.* **66**, 277 (1999).
10. S. V. Lysak, *Geol. Geofiz.* **43**, 791 (2002).
11. G. F. Belogolova and P. V. Koval, *J. Geochem. Explor.* **55**, 193 (1995).
12. P. V. Koval, R. Kh. Zaripov, G. V. Kalmychkov, et al., *Guidebook on Field Geoecological Excursion along the Angara River and Bratsk Reservoir "Mercury Pollution of the Bratsk Reservoir"* (Inst. Geokhim. Sib. Otd. Akad. Nauk, Irkutsk, 2000) [in Russian].
13. S. A. Sukhenko and O. F. Vasiliev, in *Global and Regional Mercury Cycles: Sources, Fluxes, and Mass Balances* (Kluwer, Dordrecht, 1996), pp. 122–123.
14. M. Leermakers, C. Meuleman, and W. Bayeys, in *Global and Regional Mercury Cycles: Sources, Fluxes, and Mass Balances* (Kluwer, Dordrecht, 1996), pp. 303–315.